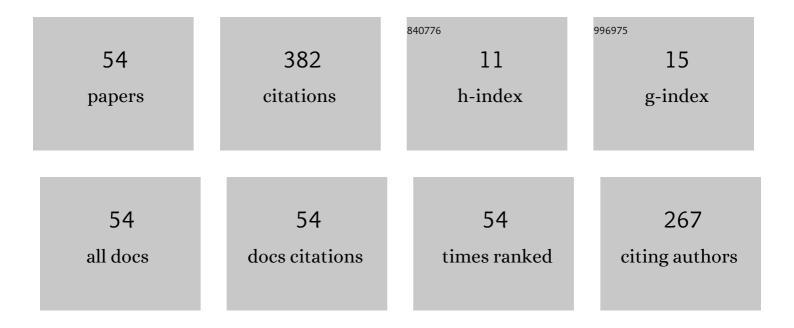
## Kazuhiro Gotoh

List of Publications by Year in descending order

Source: https://exaly.com/author-pdf/4730889/publications.pdf Version: 2024-02-01



#	Article	IF	CITATIONS
1	Hydrogen concentration at a-Si:H/c-Si heterointerfaces—The impact of deposition temperature on passivation performance. AlP Advances, 2019, 9, .	1.3	27
2	Marked enhancement of the photoresponsivity and minority-carrier lifetime of <mml:math xmlns:mml="http://www.w3.org/1998/Math/MathML"&gt;<mml:mrow><mml:mi>BaS</mml:mi><mml:msub><mml:n mathvariant="normal"&gt;i<mml:mn>2</mml:mn></mml:n </mml:msub></mml:mrow> passivated with atomic hydrogen. Physical Review Materials, 2019, 3, .</mml:math 	ni 2.4	20
3	Local Structure of High Performance TiO <i><sub>x</sub></i> Electronâ€Selective Contact Revealed by Electron Energy Loss Spectroscopy. Advanced Materials Interfaces, 2019, 6, 1801645.	3.7	15
4	Effect of hydrogen plasma treatment on the passivation performance of TiO <i>x</i> on crystalline silicon prepared by atomic layer deposition. Journal of Vacuum Science and Technology A: Vacuum, Surfaces and Films, 2020, 38, .	2.1	15
5	Application of Bayesian optimization for improved passivation performance in TiO <sub> x </sub> /SiO <sub> y </sub> /c-Si heterostructure by hydrogen plasma treatment. Applied Physics Express, 2021, 14, 025503.	2.4	15
6	Activation mechanism of TiO <i> <sub>x</sub> </i> passivating layer on crystalline Si. Applied Physics Express, 2018, 11, 102301.	2.4	14
7	Effects of evaporation vapor composition and post-annealing conditions on carrier density of undoped BaSi <sub>2</sub> evaporated films. Japanese Journal of Applied Physics, 2020, 59, SFFA05.	1.5	13
8	Atomic hydrogen passivation for photoresponsivity enhancement of boron-doped p-BaSi2 films and performance improvement of boron-doped p-BaSi2/n-Si heterojunction solar cells. Journal of Applied Physics, 2020, 127, .	2.5	13
9	Improved conversion efficiency of p-type BaSi <sub>2</sub> /n-type crystalline Si heterojunction solar cells by a low growth rate deposition of BaSi <sub>2</sub> . AIP Advances, 2022, 12, 045115.	1.3	13
10	Development of spin-coated copper iodide on silicon for use in hole-selective contacts. Energy Procedia, 2017, 124, 598-603.	1.8	12
11	Evidence of solute PEDOT:PSS as an efficient passivation material for fabrication of hybrid c-Si solar cells. Sustainable Energy and Fuels, 2019, 3, 1448-1454.	4.9	12
12	Activation energy of hydrogen desorption from high-performance titanium oxide carrier-selective contacts with silicon oxide interlayers. Current Applied Physics, 2021, 21, 36-42.	2.4	12
13	Fabrication of heterojunction crystalline Si solar cells with BaSi <sub>2</sub> thin films prepared by a two-step evaporation method. Japanese Journal of Applied Physics, 2021, 60, 105503.	1.5	12
14	Silicon Nanowire Heterojunction Solar Cells with an Al2O3 Passivation Film Fabricated by Atomic Layer Deposition. Nanoscale Research Letters, 2019, 14, 99.	5.7	11
15	Fabrication of a Silicon Nanowire Solar Cell on a Silicon-on-Insulator Substrate. Applied Sciences (Switzerland), 2019, 9, 818.	2.5	11
16	Silicon Nanocrystals Embedded in Nanolayered Silicon Oxide for Crystalline Silicon Solar Cells. ACS Applied Nano Materials, 2022, 5, 1820-1827.	5.0	11
17	Improving the photoresponse spectra of BaSi2 layers by capping with hydrogenated amorphous Si layers prepared by radio-frequency hydrogen plasma. AIP Advances, 2018, 8, 055306.	1.3	10
18	Undoped p-type BaSi <sub>2</sub> emitter prepared by thermal evaporation and post-annealing for crystalline silicon heterojunction solar cells. Applied Physics Express, 2020, 13, 051002.	2.4	10

KAZUHIRO GOTOH

#	Article	IF	CITATIONS
19	Zn <sub>1–<i>x</i></sub> Ge <sub><i>x</i></sub> O <sub><i>y</i></sub> Passivating Interlayers for BaSi <sub>2</sub> Thin-Film Solar Cells. ACS Applied Materials & Interfaces, 2022, 14, 13828-13835.	8.0	10
20	Boron-doped p-BaSi2/n-Si solar cells formed on textured n-Si(0 0 1) with a pyramid structure consisting of {1 1 1} facets. Journal of Crystal Growth, 2017, 475, 186-191.	1.5	9
21	Impact of size distributions of Ge islands as etching masks for anisotropic etching on formation of anti-reflection structures. Japanese Journal of Applied Physics, 2019, 58, 045505.	1.5	9
22	Significant enhancement of photoresponsivity in As-doped n-BaSi <sub>2</sub> epitaxial films by atomic hydrogen passivation. Applied Physics Express, 2020, 13, 051001.	2.4	8
23	Mechanisms of carrier lifetime enhancement and conductivity-type switching on hydrogen-incorporated arsenic-doped BaSi2. Thin Solid Films, 2021, 724, 138629.	1.8	8
24	Optical and structural studies of highly uniform Ge quantum dots on Si (001) substrate grown by solid-source molecular beam epitaxy. Journal of Crystal Growth, 2013, 378, 439-441.	1.5	7
25	Effect of substrate type on the electrical and structural properties of TiO2 thin films deposited by reactive DC sputtering. Journal of Crystal Growth, 2018, 491, 120-125.	1.5	7
26	Fabrication of light-trapping structure by selective etching of thin Si substrates masked with a Ge dot layer and nanomasks. Japanese Journal of Applied Physics, 2018, 57, 08RF09.	1.5	7
27	Impact of deposition of indium tin oxide double layers on hydrogenated amorphous silicon/crystalline silicon heterojunction. AIP Advances, 2020, 10, 065008.	1.3	7
28	Fabrication of Silicon Nanowire Metal-Oxide-Semiconductor Capacitors with Al2O3/TiO2/Al2O3 Stacked Dielectric Films for the Application to Energy Storage Devices. Energies, 2021, 14, 4538.	3.1	7
29	Application of Bayesian optimization for high-performance TiO /SiO /c-Si passivating contact. Solar Energy Materials and Solar Cells, 2021, 230, 111251.	6.2	7
30	Tuning the Electrical Properties of Titanium Oxide Bilayers Prepared by Atomic Layer Deposition at Different Temperatures. Physica Status Solidi (A) Applications and Materials Science, 2019, 216, 1900495.	1.8	6
31	Passivation mechanism of the high-performance titanium oxide carrier-selective contacts on crystalline silicon studied by spectroscopic ellipsometry. Japanese Journal of Applied Physics, 2021, 60, SBBF04.	1.5	6
32	Impact of chemically grown silicon oxide interlayers on the hydrogen distribution at hydrogenated amorphous silicon/crystalline silicon heterointerfaces. Applied Surface Science, 2021, 567, 150799.	6.1	6
33	Effect of the Niobium-Doped Titanium Oxide Thickness and Thermal Oxide Layer for Silicon Quantum Dot Solar Cells as a Dopant-Blocking Layer. Nanoscale Research Letters, 2020, 15, 39.	5.7	6
34	Epitaxial growth of SiGe on Si substrate by printing and firing of Al–Ge mixed paste. Japanese Journal of Applied Physics, 2019, 58, 045504.	1.5	5
35	Effect of forming gas annealing on hydrogen content and surface morphology of titanium oxide coated crystalline silicon heterocontacts. Journal of Vacuum Science and Technology A: Vacuum, Surfaces and Films, 2020, 38, 022415.	2.1	5
36	Impact of boron incorporation on properties of silicon solar cells employing p-type polycrystalline silicon grown by aluminum-induced crystallization. Japanese Journal of Applied Physics, 2018, 57, 08RB12.	1.5	3

Kazuhiro Gotoh

#	Article	IF	CITATIONS
37	Improved Performance of Titanium Oxide/Silicon Oxide Electronâ€5elective Contacts by Implementation of Magnesium Interlayers. Physica Status Solidi (A) Applications and Materials Science, 2021, 218, 2100296.	1.8	3
38	Effect of deposition rate on the characteristics of Ge quantum dots on Si (001) substrates. Thin Solid Films, 2014, 557, 80-83.	1.8	2
39	Simulation study on lateral minority carrier transport in the surface inversion layer of the p-aSi:H/i-aSi:H/cSi heterojunction solar cell. Japanese Journal of Applied Physics, 2021, 60, 026503.	1.5	2
40	Fabrication of BaSi <sub>2</sub> homojunction diodes on Nb-doped TiO <sub>2</sub> coated glass substrates by aluminum-induced crystallization and two-step evaporation method. Japanese Journal of Applied Physics, 2022, 61, SC1029.	1.5	2
41	Strain-compensated Ge/Si1â^C quantum dots with Si mediating layers grown by molecular beam epitaxy. Journal of Crystal Growth, 2015, 425, 167-171.	1.5	1
42	Deposition and Characterization of Si Quantum Dot Multilayers Prepared by Plasma Enhanced Chemical Vapor Deposition using SiH <inf>4</inf> and CO <inf>2</inf> Gases. , 2018, , .		1
43	Synthesis of Mg <sub>2</sub> Si thin film by thermal treatment under inert gas atmosphere and evaluation of film quality. Japanese Journal of Applied Physics, 2020, 59, SFFB03.	1.5	1
44	Surface inversion layer effective minority carrier mobility as one of the measures of surface quality of the p-aSi:H/i-aSi:H/cSi heterojunction solar cell. Japanese Journal of Applied Physics, 2020, 59, SGGF06.	1.5	1
45	Solar Cells Application of p-type poly-Si Thin Film by Aluminum Induced Crystallization. , 2017, , .		0
46	Fabrication of Cul/a-Si:H/c-Si Structure for Application to Hole-selective Contacts of Heterojunction Si Solar Cells. , 2017, , .		0
47	Local Structure of High Performance TiO <inf>x</inf> Passivating Layer Revealed by Electron Energy Loss Spectroscopy. , 2018, , .		0
48	Application of light trapping structure using Ge dot mask by alkaline etching to heterojunction solar cell. , 2018, , .		0
49	Photoresponsivity improvement of BaSi <inf>2</inf> epitaxial films by capping with hydrogenated amorphous Si layers by radio-frequency <inf>2</inf> plasma. , 2018, , .		0
50	Development of the Passivation Layer For P-type Cul Thin Film Fabricated by the 2-step Method as the Novel Hole Selective Contact of Silicon Heterojunction Solar Cells. , 2018, , .		0
51	Significant improvement on electrical properties of BaSi2 due to atomic H passivation by radio-frequency plasma. , 2019, , .		0
52	Realization of the Crystalline Silicon Solar Cell Using Nanocrystalline Transport Path in Ultra-thin Dielectrics for Reinforced Passivating Contact. , 2021, , .		0
53	Work function of indium oxide thin films on p-type hydrogenated amorphous silicon. , 2020, , .		0
54	Fabrication of silicon-nanocrystals-embedded silicon oxide passivating contacts. , 2020, , .		0